Hydrodynamic Computational Analysis for Propeller

Yodchai Tiaple and Pongsan Twinprawate

Department of Maritime Engineering, Faculty of International Maritime Studies, Kasetsart University, Sriracha Campus

Abstract

A propeller can hugely result in high fuel consumption efficiency for a boat. The study objective is to investigate hydrodynamic behaviour for designed propeller via three dimensional modelling. The propeller geometry is formed in three dimension by defining skew, pitch, chord, rake and thickness. These parameters are used to compute geometry at each radius of propeller in order to achieve hydrofoil section. Then, its performance is simulated by using computational fluid dynamics (CFD). The results can show openwater characteristic which is very important for selecting the operating point, propeller dimension and rotation at the high efficiency point.

Keywords : Marine propeller, Openwater characteristics, Hydrodynamics, CFD

1. Introduction

The ship business including cargo ships, fisheries and passenger boat has been struggled over the last few years due to high fuel cost. Since this trend seems to last long, most of companies are focusing on how to improve fuel consumption efficiency and fuel usage reduction [1]. The propulsion system development is one of priorities since it can affect the boat efficiency more than other systems. The ship propeller can increase or decrease fuel consumption, depending on its performance. Therefore, operated propeller in optimum efficiency point yields fuel saving up to 17% [2].

The complexity of propeller geometry is a major obstacle for design. Its shape is normally formed as cylindrical blade line, and various parameters is applied to draw its profile; however, high accuracy and design technology are required for better performance although the primary and standard data is still used for basic design. In the past, the engineer modifies each propeller from the basic design, but the efficiency has found dropping when it is used for real.

The propeller performance prediction has been studied in different methods such as experiment and numerical simulations by BEM and CFD. The experiment is carried out by using cavitation tunnel. It simulates the hydrodynamic behaviour in turbulence flow, while the Laser Doppler Velocimetry (LDV) or Particle Image Velocimetry (PIV) [3] measures pressure and velocity of fluid. However, this technique is expensive for single test and it is a huge disadvantage. In the mean time, numerical simulation has been continuously developed particular the application of inviscid potential flow. The BEM technique developed from Hess and Smith [4] predicts performance via singularity distribution on surface panel. Such technique can analyse the flow from propeller and shortening computation time; however, the difficulty appears since

the surface panel construction at wake vortex is sophisticated.

The objective of this study is to predict the performance of a new designed propeller. First, the 3D propeller geometry can be created from designed parameters using mathematic equations. Then its performance is simulated using computational fluid dynamics (CFD).

2. Propeller Design

The 3D propeller geometry can be drawn along the helical line axis as shown in figure 1. A helix occurs when the plane rotates clockwise or anti clockwise and the point P is moving away from the observer looking along the axis of rotation. The different cross sections depending on each radius are called the hydrofoil cross section which consists of two edges: Leading edge (L.E.), and Tailing edge (T.E.). The essential parameters as shown in the figure 1 are computed by defining P point at each section coordinate. From the point P, the geometry coordinates can be defined by using equation 1 [5].

$$
\begin{aligned}
x_P &= -\left[i_G + r\theta_s \tan(\theta_{nt})\right] + (0.5c - x_c)\sin(\theta_{nt}) + y_c \cos(\theta_{nt}) \\
y_P &= -r \cdot \sin\left(\frac{\left[(0.5c - x_c)\cos(\theta_{nt}) - y_c \sin(\theta_{nt})\right]}{r} - \theta_s \right) \\
z_P &= \; r \cdot \cos\left(\frac{\left[(0.5c - x_c)\cos(\theta_{nt}) - y_c \sin(\theta_{nt})\right]}{r} - \theta_s \right)
\end{aligned} \quad (1)
$$

where i_G is generator rake, θ_s is skew θ_{nt} is pitch angle and c is the chord length, while y_c is camber line, plus and minus, with half of the thickness t at position of given cross section for upper and lower blade surface respectively.

This study was based on data of Chaophraya passenger boat as shown in figure 2 as a case study for simulating characteristics of suitable propeller. The dimension of the boat consisted of 30.75 m length, 4 m width and 0.5 draft, while its weight was 28.1Tons. Its 265 kW engine produced average speed at 15 knots at 900 rpm, and the top speed was 17 knots at 1100 rpm. The propeller diameter was 0.813 m with three blades.

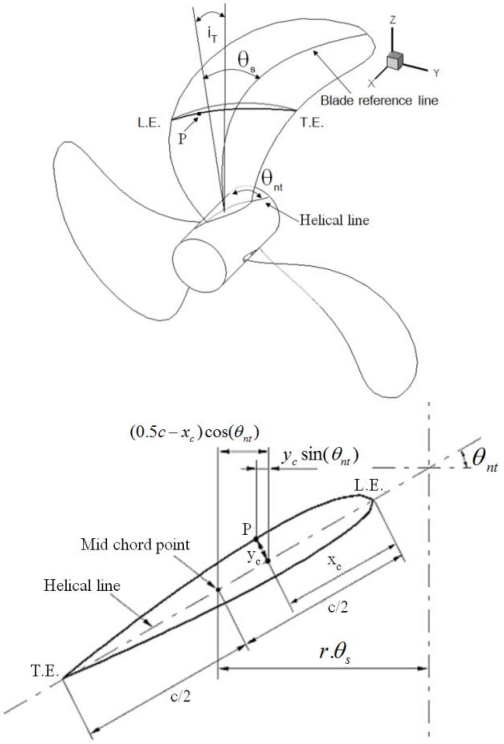

Figure 1 Parameters for defining propeller geometry [6]

The parameters were applied to equation 1 in order to create the 3D propeller geometry: its diameter was set as 0.813 m and hub was 0.15D for three blades. The rake angle was 15^{o}, while the camber line function was selected as NACA a=0.8 then, the skew, pitch, chord and thickness distributions at any radius as shown in figure 3 were applied in equation 1. Eventually, the 3D propeller geometry was created as shown in figure 4.

Figure 2 Chaopharya passenger boat

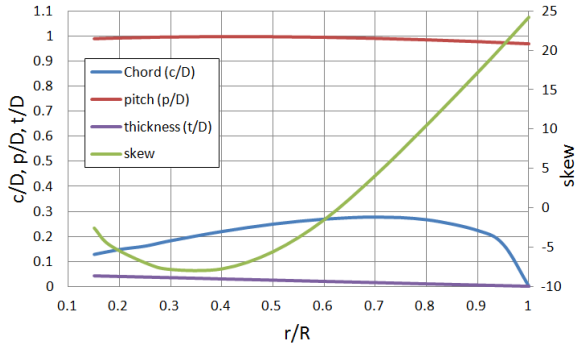

Figure 3 Pitch, Chord, Thickness and Skew distribution of propeller

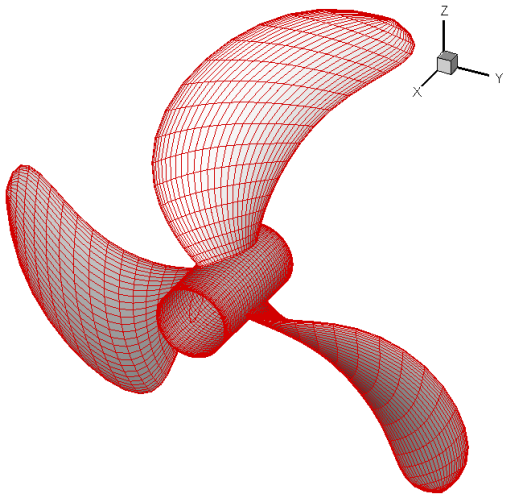

Figure 4 3D propeller geometry

3. Computational Method

The modified Navier-Stokes equations (NESs) called Reynolds-Averaged Navier-Stokes (RANS) equations were used for flow governing equation as: [7]

$$\frac{\partial \rho}{\partial t}+\frac{\partial(\rho \cdot u_i)}{\partial x_i}=0 \tag{2}$$

$$\frac{\partial(\rho \cdot u_i)}{\partial t}+\frac{\partial(\rho \cdot u_i \cdot u_j)}{\partial x_j} = -\frac{\partial p}{\partial x_i}+\frac{\partial}{\partial x_j}\left[\mu \cdot\left(\frac{\partial u_i}{\partial u_j}+\frac{\partial u_j}{\partial u_i}-\frac{2}{3}\cdot\delta_{ij}\cdot\frac{\partial u_l}{\partial x_l}\right)\right]+\tau_{ij} \tag{3}$$

The additional unknown terms were named Reynolds Stress and defined as

$$\tau_{ij}=\rho\cdot\overline{u_i'\cdot u_j'}$$

According to Boussinesq hypothesis the derived Reynolds stress became

$$\tau_{ij}=\mu_t\cdot\left(\frac{\partial u_i}{\partial x_j}+\frac{\partial u_j}{\partial x_i}\right)-\frac{2}{3}\cdot\left(\rho\cdot k+\mu_t\cdot\frac{\partial u_i}{\partial x_i}\right)\cdot\delta_{ij} \tag{4}$$

From the $k-\varepsilon$ turbulence model, the turbulence viscosity term (μ_t) was

$$\mu_t=\rho\cdot C_\mu\cdot\frac{k^2}{\varepsilon}$$

The equation was transformed as k and ε function due to turbulent flow model as:

$$\rho\cdot\frac{Dk}{Dt}=\frac{\partial}{\partial x_i}\cdot\left[\left(\mu+\frac{\mu_t}{\sigma_k}\right)\cdot\frac{\partial k}{\partial x_j}\right]+\mathrm{P}-\rho\cdot\varepsilon \tag{5}$$

and

$$\rho\cdot\frac{D\varepsilon}{Dt}=\frac{\partial}{\partial x_j}\cdot\left[\left(\mu+\frac{\mu_t}{\sigma_\varepsilon}\right)\cdot\frac{\partial\varepsilon}{\partial x_i}\right]+C_{1\varepsilon}\cdot\frac{\varepsilon}{k}\cdot P-C_{2\varepsilon}\cdot\rho\cdot\frac{\varepsilon^2}{k} \tag{6}$$

where P was production of turbulent kinetic energy and $\sigma_k, \sigma_\varepsilon, C_{1\varepsilon}$ and $C_{2\varepsilon}$ were constant

From the $k-\omega$ Turbulence model, the turbulent viscosity term was

$$\mu_t=\rho\cdot\frac{k}{\omega}$$

The equation was transformed as k and ω function due to turbulent flow model as:

$$\rho\cdot\frac{Dk}{Dt}=\frac{\partial}{\partial x_i}\cdot\left[(\mu+\sigma\cdot\mu_t)\cdot\frac{\partial k}{\partial x_j}\right]+\mathrm{P}-\beta\cdot\rho k\omega \tag{7}$$

and

$$\rho\cdot\frac{D\omega}{Dt}=\frac{\partial}{\partial x_j}\cdot\left[(\mu+\sigma\mu_t)\cdot\frac{\partial\omega}{\partial x_i}\right]+\alpha P\frac{\omega}{k}-\beta\rho\omega^2 \tag{8}$$

where P was production of turbulent kinetic energy and α, β and σ were constant.

The commercial CFD code, Fluent V.6.3, was used to investigate hydrodynamic behaviour for designed propeller. The model was composed of the cylindrical outer and inner domains. The propeller was placed 2.5D from velocity inlet and 10D from outlet as shown in figure 5.

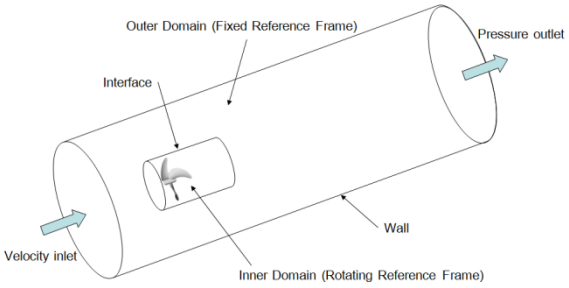

Figure 5 Boundary condition

The mesh of modelled propeller was defined by Gambit program in unstructured mesh mode because it was simple and convenient; moreover, its solution also indicated small errors [8]. This simulation was using rotating reference frame model. The velocity inlet condition was set for upstream inlet surface and the pressure outlet condition was set for downstream outlet surface as shown in figure 5. The interface boundary condition was set on the intersect surface of the outer and inner domains. The outer domain was stationary, while the inner domain was operated at the constant rotational speed. The surface of blade and hub were no-slip condition. The simulation was set to be steady flow and k-ε and k-ω turbulence models were selected for calculation and the residual monitor was 10^{-4}. The flow model was applied in single phase without cavitation effect.

4. Result and discussion

The results from the model were compared to result of H. R. Shin and J. Shitalkumar's P5168 propeller [9]. The P5168 was five-blade controllable-pitch with 0.4027m diameter. It was modelled by tetrahedral mesh with 560,000 grids. The model was performed at $J=V_A/(nD)=0.98,\ 1.10,\ 1.27,\ 1.51$ where V_A was inlet velocity, n was rotation per second (rps) and D was propeller diameter. The k-ε and k-ω models were chosen to study pressure distribution at front and back of the blade as shown in figure 6. The pressure was low at leading edge at suction side, while the high pressure was found at leading edge at pressure side. Figure 7 indicated K_T and K_Q comparing to H. R. Shin and J. Shitalkumar [9]. The results showed consistency at J=1.0 - 1.3, while showed lower at J=1.5; however, the result from k-ω model and k-ε model indicated consistency over J=1.0 - 1.5. K_T and K_Q were thrust coefficient and torque coefficient respectively, and they can be written in non-dimensional equation as:

$$K_T = \frac{T}{\rho \cdot n^2 \cdot D^4} \tag{9}$$

$$K_Q = \frac{Q}{\rho \cdot n^2 \cdot D^5} \tag{10}$$

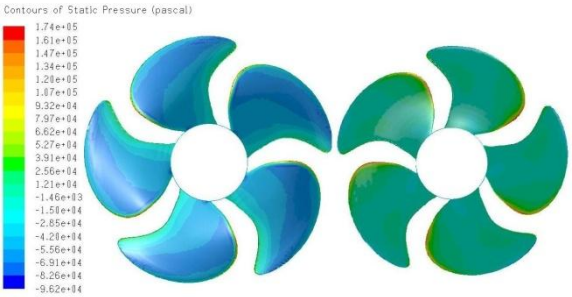

Figure 6 Pressure distributions on P5168

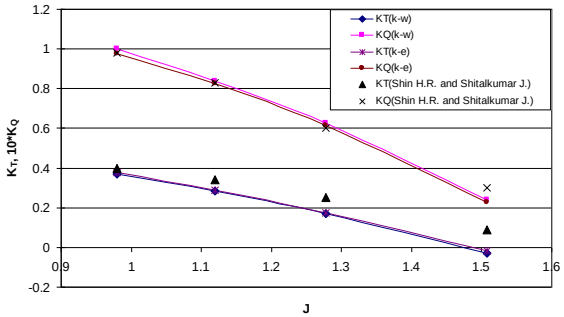

Figure 7 Comparison of predicted K_T and K_Q of P5168

where T was thrust (N), Q was torque (N.m), D was diameter. The propeller efficiency without ship body effect called openwater characteristics was computed from thrust and torque coefficient and advance number as:

$$\eta_0 = \frac{T \cdot V_A}{2\pi \cdot n \cdot Q} = \frac{K_T \cdot \rho \cdot n^2 \cdot D^4}{K_Q \cdot \rho \cdot n^2 \cdot D^5} \cdot \frac{V_A}{2\pi \cdot n} = \frac{K_T}{K_Q} \cdot \frac{J}{2\pi} \quad (11)$$

For investigated propeller of Chaophraya passenger boat, it was also modelled by tetrahedral mesh. Figure 8 showed computational grids. Prior to the analysis of propeller, the optimal number of grids had to be determined. Hence, a preliminary grid dependency was tested with number of grids ranging from 550,728 to 933,829 (see figure 9) and 810,497-nodes were selected as the optimum number of grids. The calculation was carried out from J = 0.2-1.0. The pressure distribution at front and back of the blade was simulated by using k-ε model as shown in figure 10. The path line at tip of the blade simulated by k-ε model at J=0.6 was shown in figure 11.

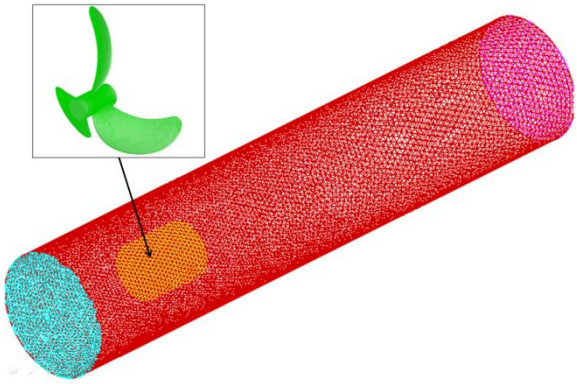

Figure 8 Computational grids

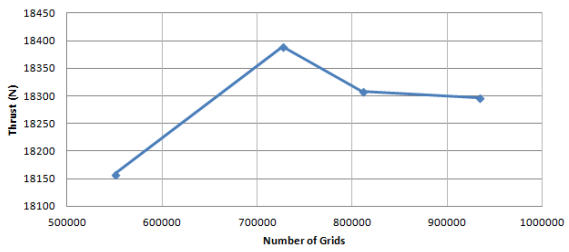

Figure 9 Grid dependency test results

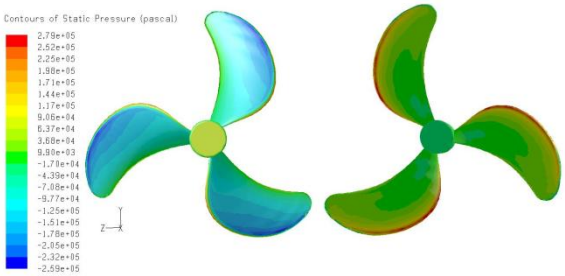

Figure 10 Pressure distribution on propeller

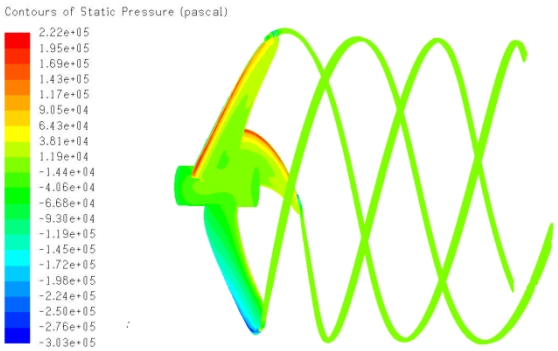

Figure 11 Path line at tip of tailing blade

In order to investigate loads on the blade, C_p on the blade at the same radius (r=0.7R) was computed by using k-ε model at J=0.6, 0.7 0.8 and 1.0 were shown in figure 12 as equation 12.

$$C_P = \frac{(P - P_\infty)}{\frac{1}{2}\rho V^2} \quad (12)$$

where P_∞ was atmospheric pressure and ρ was water density.

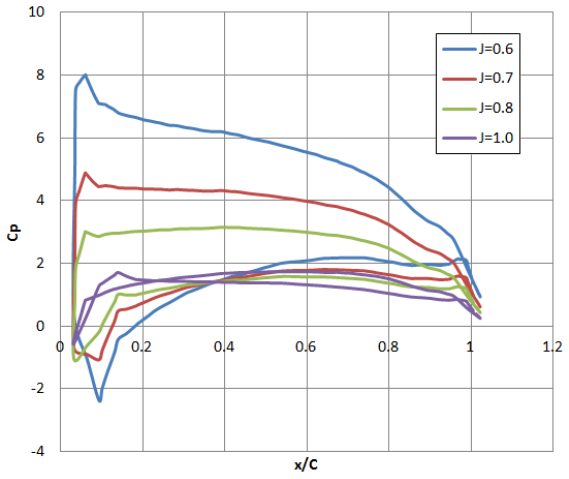

Figure 12 Comparison of pressure distribution at r=0.7R

Openwater characteristics can be simulated by setting the D=0.813 m, n=1100 rpm and adjusting velocity for J ranging from 0.1 to 1.0. Figure 13 shows openwater characteristics (K_T, K_Q and η_0) of the propeller. The comparison between k-ε and k-ω models showed that the result from k-ω model was lower than k-ε model all over the J range.

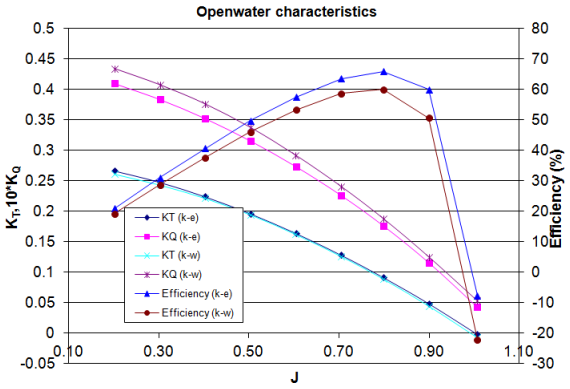

Figure 13 Comparison between K_T, K_Q and η_0

5. Conclusion

The flow analysing through propeller is sophisticated particularly at turbulent mode; this yields complication for propeller design. This study has developed method for propeller design to become more practical. The 3D propeller shape can be drawn by defining skew, pitch, chord, rake and thickness. With these parameters, each component of propeller is easy to adjust; moreover, the 3D geometry can be formed easily. Then, the CFD is used to simulate openwater characteristics of the 3D propeller.

By using the present method, it is more convenient and takes lesser time to design and develop a propeller suitable for each boat than using an usual experimental method. The openwater characteristic of propeller is important to boat speed. The appropriate boat speed and propeller rotational speed affect directly the propulsion performance resulting in improved fuel economy.

6. Acknowledgement

The authors gratefully thank Centre of excellence Kasetsart Univeristy for funding contribution and also Chaophraya speed boat company for allowing propeller installation and testing.

7. References

[1] B. Sazetak, “New Technologies for Reducing Fuel Consumption in Marine Vehicles”, XVI Symposium SORTA2004.

[2] K. Hochkirch and V. Bertran, “Options for Fuel Saving for Ships”.

[3] G. Calcagno et al, “The INSEAN E779a Propellr Test Case: a Database for CFD Valiadtion”.

[4] J.L. Hess, and A.M.O. Smith, “Calculation of Non-lifting Potential Flow About Arbitrary 3-Diamensional Bodies”, Journal of Ship Research, 8(2), pp.22-44, 1964.

[5] J.S. Carlton, Marine propellers & propulsion, Butterworth-Heinemann Ltd, 1994.

[6] S. Phoemsapthawee, “Design of Marine Propeller Using Boundary Element Method”, Master Thesis, King’s Mongkut Instute Technology North Bangkok, 2001

[7] T. J. Chung, Computational fluid dynamics, Cambridge University Press, 2002.

[8] J. Kulczyk et al, “Analysis of Screw Propeller 5119 Using the Fluent System”, Archives civil and Mechanical Engineering Vol. VII No.4, 2007.

[9] H.R. Shin and J. Shitalkumar, “Computational Validation for Flow Around a Marine Propeller Using Unstrutured Mesh Based Navier-Stokes Solvers”, JSME International Journal, Series B, Vol.48, No.3, pp 562-570, 2005.